



SHARPENS YOUR THINKING

## Boundary Extraction in Images Using Hierarchical Clustering-based Segmentation

SELVAN, Arul

Available from Sheffield Hallam University Research Archive (SHURA) at:

<http://shura.shu.ac.uk/4050/>

---

This document is the author deposited version. You are advised to consult the publisher's version if you wish to cite from it.

### Published version

SELVAN, Arul (2011). Boundary Extraction in Images Using Hierarchical Clustering-based Segmentation. In: The 3rd BMVC UK Student Workshop: Friday September 2, Dundee, UK, 2nd September, 2011.. (Submitted)

---

### Repository use policy

Copyright © and Moral Rights for the papers on this site are retained by the individual authors and/or other copyright owners. Users may download and/or print one copy of any article(s) in SHURA to facilitate their private study or for non-commercial research. You may not engage in further distribution of the material or use it for any profit-making activities or any commercial gain.

# Boundary Extraction in Images Using Hierarchical Clustering-based Segmentation

Arul N. Selvan<sup>1</sup>  
a.n.selvan@SHU.ac.uk  
<http://www.shu.ac.uk/research/meri/mmv1/research/projects/medical/index.html>

<sup>1</sup> Materials & Engineering Research Inst.  
Sheffield Hallam University,  
Sheffield. S1 1WB. UK.

---

## Abstract

Hierarchical organization is one of the main characteristics of human segmentation. A human subject segments a natural image by identifying physical objects and marking their boundaries up to a certain level of detail [1]. Hierarchical clustering based segmentation (HCS) process mimics this capability of the human vision. The HCS process automatically generates a hierarchy of segmented images. The hierarchy represents the continuous merging of similar, spatially adjacent or disjoint, regions as the allowable threshold value of dissimilarity between regions, for merging, is gradually increased. HCS process is unsupervised and is completely data driven. This ensures that the segmentation process can be applied to any image, without any prior information about the image data and without any need for prior training of the segmentation process with the relevant image data.

The implementation details of HCS process have been described elsewhere in the author's work [2]. The purpose of the current study is to demonstrate the performance of the HCS process in outlining boundaries in images and its possible application in processing medical images.

## 1 Introduction

Segmentation can be thought as a process of grouping visual information, where the details are grouped into objects, objects into classes of objects, etc. Thus, starting from the composite segmentation, the perceptual organization of the image can be represented by a tree of regions, ordered by inclusion. The root of the tree is the entire scene, the leaves are the finest details and each region represents an object at a certain scale of observation [1]. Since the early days of computer vision, the hierarchical structure of visual perception has motivated clustering techniques to segmentation [3], where connected regions of the image domain are classified according to an inter-region dissimilarity measure.

Hierarchical Clustering-based Segmentation (HCS) implements the traditional bottom-up approach, also called agglomerative clustering [4], where the regions of an initial partition are iteratively merged. HCS procedure automatically generates a hierarchy of segmented images. The hierarchy of segmented images is generated by partitioning an image into its constituent regions at hierarchical levels of allowable dissimilarity between its different regions. At any particular level in the hierarchy, the segmentation process will cluster together all the pixels and/or regions which have dissimilarity among them less than or equal to the dissimilarity allowed for that level.

It should be noted that HCS process is quite different from Hierarchical image segmentation methods discussed, for example, in [5]. The hierarchy in the study [5] refers

to the multi-resolution hierarchy in scale space. Also HCS process, unlike other segmentation methods like [6], [7] and [8], is not an iterative optimization process. Instead at each level HCS process yields an optimized segmentation output related to the dissimilarity allowed for that level.

Details of the implementation of the HCS process are described in the author's work in [2]. The purpose of this paper is two fold firstly to present the results of the objective evaluation of the performance of HCS process as a segmentation tool and secondly to present the possibility of how HCS process can be used as a computer aided monitoring (CAM) tool to assist radiologists to monitor abnormalities in X-ray mammograms.

The rest of the paper is organized as follows. Firstly the operation of the HCS process is outlined. Also the facilities offered by the GUI to display the HCS output is discussed. Secondly the performance of the HCS process is evaluated. Finally the success of HCS in segmenting medical images and using HCS process as an aid for radiologists are discussed.

## 2 Overview of the HCS Process

Following is a high-level description of the HCS process [2] (See Figure 1 for a flow chart representation) :

1. Give each pixel in the image a region label as follows :
  - If an initial segmentation of the image is available, label each pixel according to this pre-segmentation. The initial segmentation can be obtained by prior class information (for e.g. based on the user information).
  - If no initial segmentation is available, label each pixel as a separate region.
  - Set current dissimilarity allowed between regions, *dissimilarity\_allowed*, equal to zero.
2. Calculate the dissimilarity value, (*dissimilarity\_value*), between all pairs of regions in the image.
  - Set *threshold\_value* equal to the smallest *dissimilarity\_value*.
3. If the *threshold\_value* found, in step 2, is less than or equal to the current *dissimilarity\_allowed* value, then merge all those regions having *dissimilarity\_value*, between them, less than or equal to the *threshold\_value*.
  - Otherwise go to step 6.
4. If the number of regions merged in step 3 is greater than 0, then reclassify the pixels on the border of the merged regions with the rest of the regions until no more reclassification is possible. After all the possible border pixels are reclassified, among the merged regions, store the region information for this iteration as an intermediate segmentation and go to step 2.
  - Otherwise, if the number of regions merged in step 3 is equal to 0 then, go to step 5.
5. If the current number of regions in the image is less than the pre-set value, *check\_no\_regions*, then go to step 7. Otherwise, go to step 6.
6. If the current value of *dissimilarity\_allowed* is less than the maximum possible value then increase the *dissimilarity\_allowed* value by an incremental value,  $dissimilarity_allowed = dissimilarity_allowed + dissimilarity_increment$ , and go to step 2. Otherwise go to step 7.
7. Save the region information from the current iteration as the coarsest instance

The above steps ensures that the segmentation does not depend on the order in which the image regions are processed. Normally in agglomerative clustering methods the cluster structure depends on the order in which the regions are considered [4]. The brute force approach, followed by the HCS process, where only those regions with the smallest overall dissimilarity are merged in each step, is the only solution to overcome this effect [9].

The feature measure used by the HCS process to estimate the similarity is the actual distribution of the pixel values in a region surrounding the locations. This technique may be considered to work in a way similar to the human visual system where features for texture (region) segmentation are not consciously computed [10].

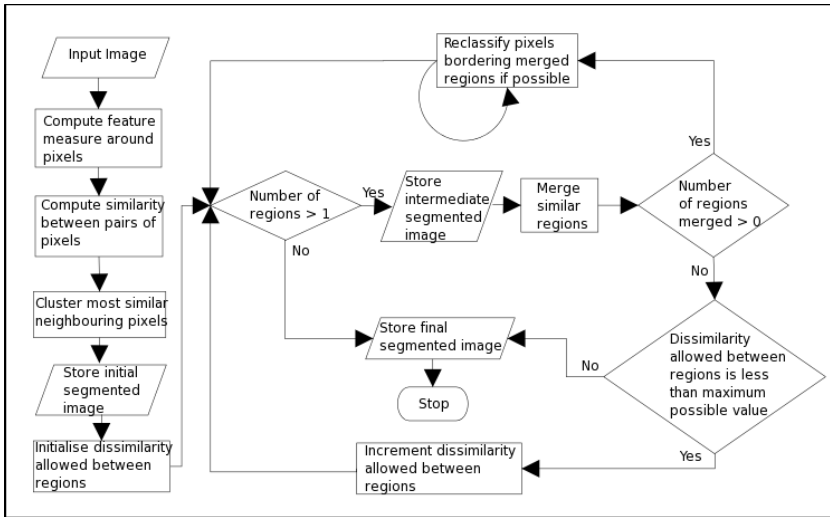


Figure 1: Flow chart illustrating the different operations of the HCS process [2]

## 2.1 Graphical User Interface (GUI) for Displaying HCS Results

The HCS process generates a hierarchy of segmentation results, associated with a set of dissimilarity values. The segmentation output is stored at the end of the HCS processing. Subsequently the GUI can be used to reproduce the resulting segmentation images associated with a dissimilarity value instantaneously. The GUI is designed in such a way as to make it easy for the user to view all the different solutions and select the most suitable. The easy viewing and scrutinizing of the segmentation output is achieved by the GUI by having the following facilities :

1. The hierarchical segmentation output can be viewed by using a slider bar giving the dissimilarity index.
2. Individual region properties like the number of pixels, the lowest, highest and average pixel value and the distribution of the pixel values within the region can be scrutinized.
3. The original image or another segmented image at a different level of dissimilarity can be compared with a segmented image by displaying them alongside each other and a dual cursor moves simultaneously on both the images.

The image shown in Figure 2 gives a screen captured image of the GUI and the user controls provided for the above listed facilities. The GUI facility will be useful for the user to choose the right segmentation to identify the regions which correspond to the healthy and diseased part of the breast tissue in X-ray mammograms (Section 3).

## 2.2 Objective Evaluation of the Performance of the HCS Process

To evaluate the performance of segmentation methods like HCS, which yield a hierarchy of boundaries, Precision-Recall curves, (Berkley benchmark) an alternative to Receiver Operating Characteristic (ROC) curve, is more suited [11]. The procedure to benchmark the performance of any boundary detecting algorithm, like HCS, is described as follows :

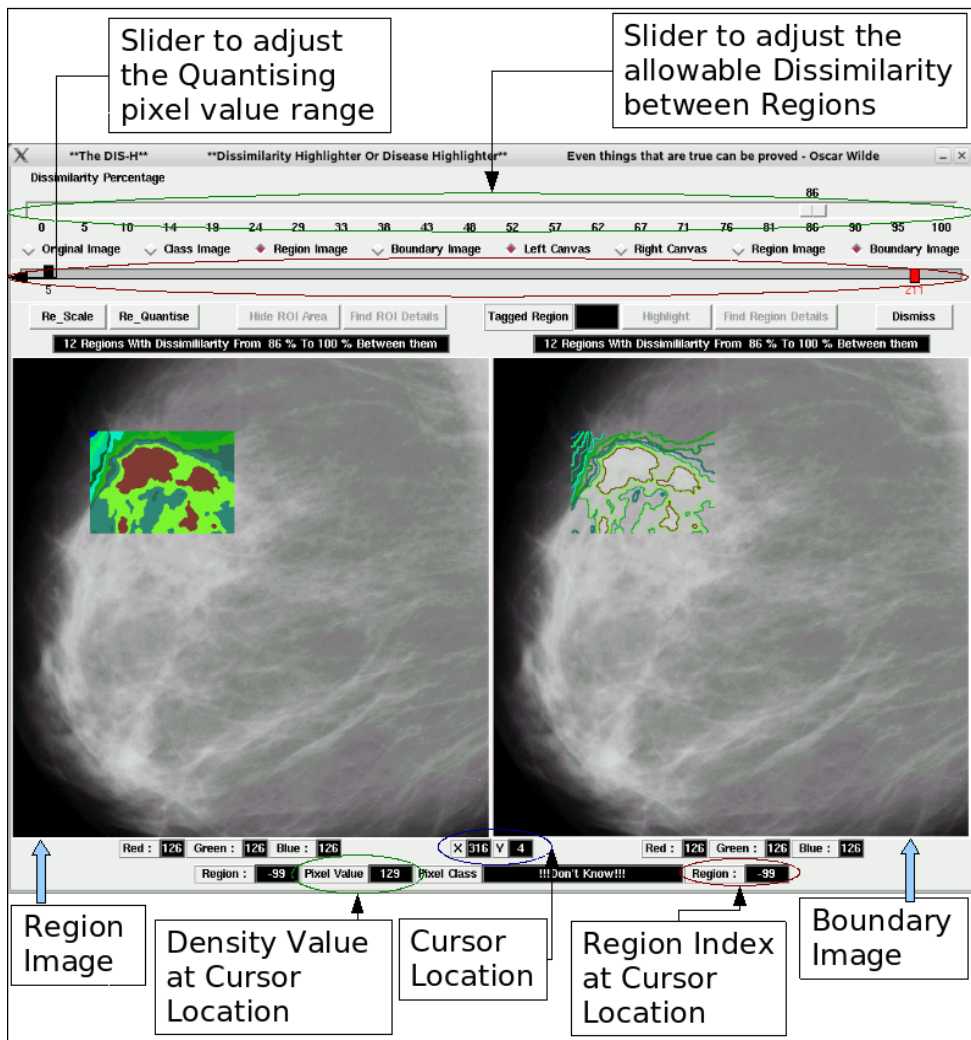


Figure 2: Annotated screen captured image of the GUI, to visualize HCS process output.

For each image a collection of human-marked boundaries, marked by different human subjects, constitutes the ground truth. The output of the boundary detecting algorithm, will be a boundary map with one pixel wide boundaries. The objective is to find out how well the algorithm's boundary map matches with that of the human subjects'.

Traditionally, one would "binarize" the boundary map by choosing some threshold. There are two problems with thresholding a boundary map: [12]

1. The optimal threshold depends on the application, and
2. Thresholding a low-level feature like boundaries is likely to be a bad idea for most applications, since it destroys much information.

For these reasons, the Berkley benchmark operates on a non-thresholded boundary map. Nevertheless, one need to threshold the boundary map in order to compare it to the ground truth boundaries, but this is done at many levels. At each level, the two quantities -- precision and recall -- are computed. In this manner the precision-recall curve for the boundary detecting algorithm is produced [12].

The performance of the boundary detecting algorithm is measured by estimating the summary statistic as follows : The F-measure, which is the harmonic mean of precision and recall is defined at all points on the precision-recall curve. The maximum F-measure value across an algorithm's precision-recall curve is its summary statistic [12].

A subset of one of the natural scenes of the Berkley database [12] (Image ID 42049) (Figure 3 a) was used to evaluate the performance of the HCS process, as discussed above. Figure 3 shows the human subjects' hand drawn boundaries (Top row) and some of the HCS process intermediate segmentation output (Bottom row). Figure 4 shows the precision and recall plot for 228 segmentation levels of the HCS process. For the HCS process the maximum F-measure value was found to be 0.82 (Figure 4).

The corresponding scores for other segmentation algorithms ranges from 0.92 [13] to 0.76 [14]. (See [12]). The algorithm which has got the highest score of 0.92 is supervised [13] while HCS process is unsupervised. Moreover the human subjects' boundaries, with which the algorithms' output is compared, outline only the major structures in the scene. For example none of the human subjects has outlined the border of the bird's legs. In contrast the HCS process has not only outlined the legs of the bird but has also outlined the subtle difference in the chest plumage of the bird (Figure 5). This outlining of subtle differences within an otherwise a homogeneous region is found very useful in highlighting dissimilarities in diagnostic images. Because tissue abnormalities, in medical images are indicated, by part of the image being dissimilar from other homogeneous areas representing healthy parts.

### 3 Medical Image Segmentation Using HCS Process

The goal of medical image segmentation is to separate the image into regions that are meaningful for a specific task. This task may, for instance, involve the detection of specific section of organs or quantitative measurements made from the images. Medical image segmentation is a difficult task because of issues such as spatial resolution, poor contrast, ill-defined boundaries, noise, or acquisition artefacts [15]. The medical images in the Figures 6 and 7 illustrate this difficulty. Figure 6 shows a CT image of a section of the brain. The image area within the region of interest (rectangular area outlined in black) is made up of three different types of regions viz. Grey matter, White matter and the stroke affected area. The stroke affected area has been outlined in white by an expert. Figure 7 shows the segmentation result obtained by Hierarchical Segmentation (HSEG) [16] which is very similar to HCS process. Figure 7 illustrates the difficulties faced by the HSEG process to segment medical images. Although the image pixels within the region of interest (ROI), have been segmented into three classes colour coded as Red (the diseased area), Green (white matter) and blue (Grey matter) it has misclassified some of the pixels not belonging to the diseased area as being diseased as well. This can be seen by the presence of red coloured pixels at the other end of the ROI outside the area outlined by the expert.

Figure 8 shows the segmentation of the same CT image (Figure 6) by the HCS process. It can be seen that the HCS process has successfully delineated the three different types of regions viz. Grey matter, White matter and the stroke affected area. Comparing the segmentation results of the HCS process Figure 8 and with that of the HSEG process Figure 7, it can be seen that the HSEG process segmentation (Figure 7) is suboptimal while the HCS process is able to achieve a smooth segmentation as can be seen in Figure 8.

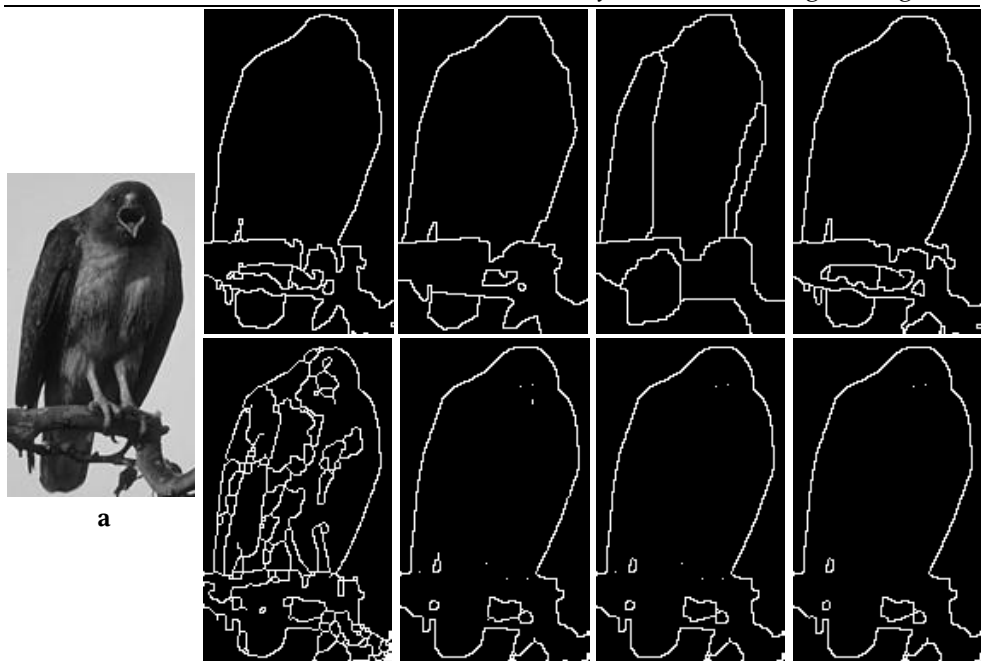


Figure 3: A natural scene from the Berkeley database (subset of Image ID 42049) (a). Top row images are boundaries, marked by 4 different human subjects. Bottom row images are the HCS process boundary output when there were 22, 15, 10 and 6 regions.

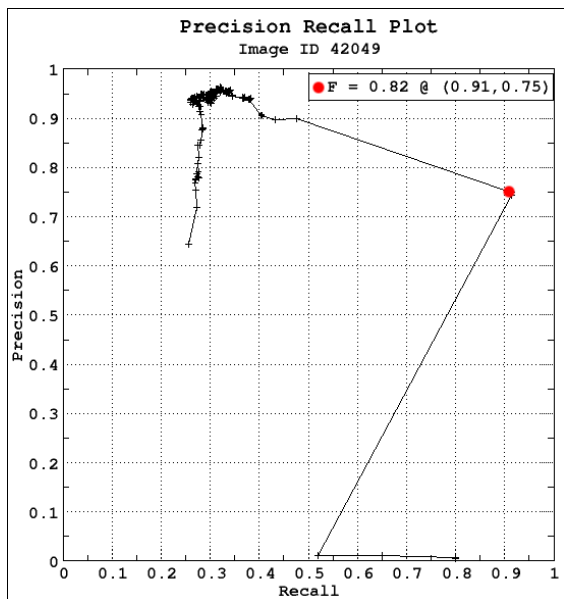


Figure 4: Precision and Recall plot for 228 levels

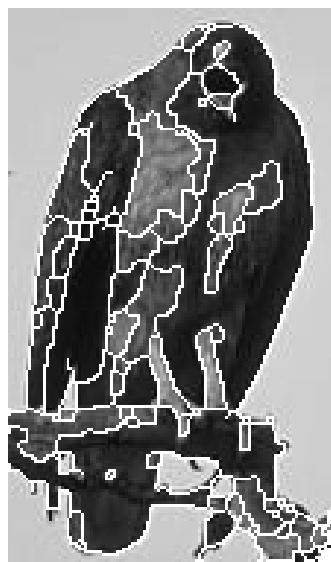


Figure 5: HCS process segmentation of the natural scene (Figure 3 a)

### 3.1 Border Pixel Re-Classification

One of the unique feature of the HCS process is the border pixel classification operation (Figure 1). Border pixel reclassification is necessary because the merging process starts





Figure 6: CT image showing the suspected area outlined in white by a neuroradiologist.

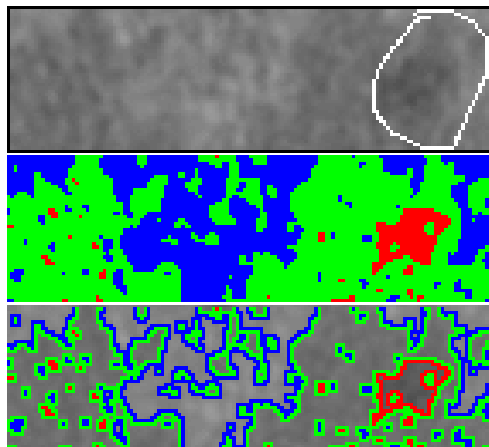


Figure 7: Segmentation of the Grey matter, White matter and Stroke affected regions and their boundaries by HSEG [16]

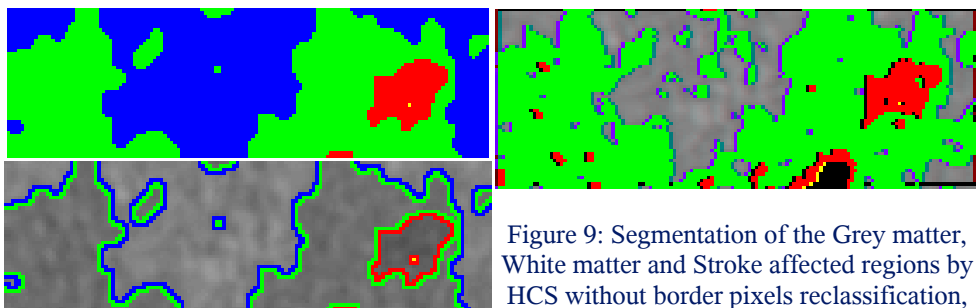


Figure 8: Segmentation of the Grey matter, White matter and Stroke affected regions and their boundaries by HCS [2]

with individual pixels and the pixels are merged to form regions and subsequently regions are merged to form bigger regions and so on. During the initial merging pixels/regions belonging to different types/classes might get merged. This could happen, for example when comparing pixels/regions over a small neighbourhood, where the dissimilarity between pixels/regions belonging to different types/classes of regions might be smaller than the dissimilarity between pixels/regions belonging to the same type/class of region because of the local in-homogeneity. However as the regions grow, during border pixel reclassification, those pixels which had been merged as a result of comparison with smaller neighbourhood might subsequently be reclassified by properly comparing them with the rest of the pixels from a larger neighbourhood.

Border pixel reclassification was considered only for those pixels on the boundary of the clusters which had been merged with other clusters. These boundary pixels were removed one at a time from their original clusters. The pixel removed was considered as a region of its own and the similarity between the one pixel region and the regions bordering it (which include the original cluster to which it belonged to) were found and the single pixel region was merged with the most similar bordering region.

Figure 9: Segmentation of the Grey matter, White matter and Stroke affected regions by HCS without border pixels reclassification, where misclassification had occurred.[2]



Figure 9 shows the intermediate segmentation results of the HCS process, performed without border pixels reclassification. In Figure 9 the pixels belonging to the larger clusters of the major classes White Matter and the infarct are coloured as Green and Red. Pixels clustered as belonging to the Grey matter class are not coloured. From Figure 9 it can be seen that the cluster belonging to the major class infarct has misclassified pixels on the other part of the image.

Comparing the segmentation output of the HSEG (Figure 7) with that obtained by HCS without border pixel reclassification (Figure 9), it can be seen that they are almost the same. Since the similarity measures adopted by the HCS and the HSEG processes may or may not be the same it can be safely assumed that border pixel reclassification plays a crucial role in obtaining a smooth segmentation.

Although only one example was shown to compare the performance of the HSEG with that of HCS. It is also shown how HCS process output is very similar to that of HSEG when HCS process does not perform border-pixel reclassification. From this it can be inferred that HCS process with border-pixel-reclassification will always give a better segmentation output when compared to HSEG.

### 3.2 HCS Process as a Computer Aided Monitoring (CAM) Tool

X-ray mammography is the most effective tool for the detection and diagnosis of breast cancer, but the interpretation of mammograms is a error-prone task. Hence, computer aids have been developed to assist the radiologist. While Computer-aided detection (CADe) systems address the problem that radiologists often miss signs of cancers, Computer-aided diagnosis (CADx) systems assist them to classify the lesions as benign or malignant [17].

This study demonstrates a novel alternative system namely computer-aided monitoring (CAM) system. The designed CAM system can be used to objectively measure the properties of suspected abnormal areas in mammograms. Thus it can be used to assist the clinician to objectively monitor abnormalities. In brief the designed CAM system works as follows : Using the approximate location and size of an abnormality, obtained from the user, the HCS process automatically identifies the more appropriate boundaries of the different regions within a region of interest (ROI), centred at the approximate location. From the set of, HCS process segmented, regions the user identifies the regions which most likely represent the abnormality and the healthy areas. Subsequently the CAM system compares the characteristics of the user identified abnormal region with that of the healthy region; to differentiate malignant from benign abnormality. An example follows.

Figure 10 shows a X-ray mammogram (mdb102) of a dense glandular breast having a malignant asymmetry class of abnormality. Using the information provided in the miniMIAS database [18] the approximate boundary of the abnormality (Red circle Figure 10 a), was located. The HCS process was applied within a ROI centred on the abnormality. Inspecting the HCS process output the user selected the region corresponding to the abnormality (Red Figures 10 b, c and d). The area within the approximate circular boundary, other than the abnormality, was selected as healthy, (Green Figure 10 d). Inspecting the HCS process output the user also selected a location, within the abnormal area, which was considered as the core of the abnormality (Yellow Figure 10 d and e). To estimate the dissimilarity between the abnormal and the healthy regions, the HCS process was applied only to the pixel locations within the abnormality (Red Figure 10 d and e) and the healthy (Green Figure 10 d and e) areas of the image. As the HCS process goes about merging similar regions within the abnormality and the healthy areas, the maximum average dissimilarity, measured between the cluster having the user tagged location (within

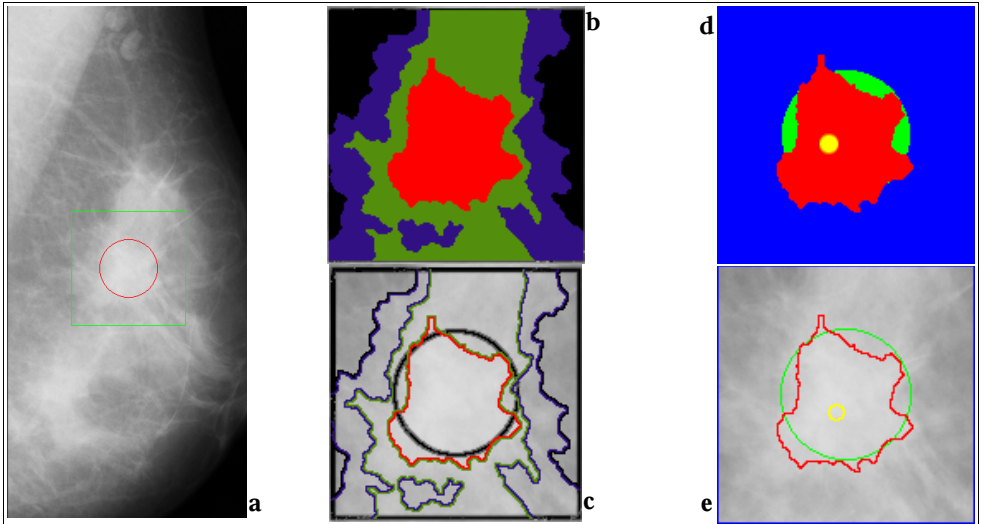


Figure 10: mini-MIAS mammogram (Image-ID mdb102) with the location and the approximate boundary of the abnormality circled in Red by the user (a). HCS process intermediate segmentation of four regions and their boundaries (b and c). Regions, and their boundaries, identified by the user as healthy (Green) and abnormal (Red) (d and e).

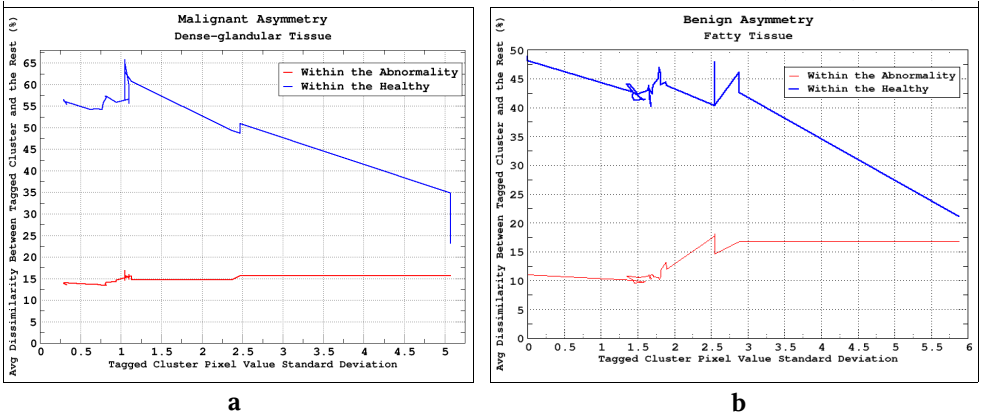


Figure 11: For mini-MIAS Mammogram images mdb102 and mdb097 graphs (a and b) showing the dissimilarity between the cluster having the user tagged location and other clusters belonging to the abnormality area and the healthy area.

the abnormality) and the clusters within the healthy region, is estimated. The heuristic used for differentiating malignant from benign abnormality is, if the value of the above estimated measure is less than fifty percent then the abnormality is benign else malignant. Graph shown in Figure 11 (a) demonstrates how the above measure and the criteria is able to classify the abnormality, under consideration, as malignant. Similarly the graph shown in Figure 11 (b) demonstrates how a benign abnormality is correctly classified.

The technique used to rate the HCS process based CAM effectiveness was to give it one malignant case and one benign case and then test its ability to determine which is which. The designed CAM process achieved 100% success rate in classifying malignant from benign asymmetric and circulant class of abnormalities in 16 mammograms from the mini-MIAS. The HCS process classifications were matched with that given in the mini-MIAS database [18].

## 4 Conclusion

Radiologists' expertise in reading diagnostic images calls for a combination of perceptual skills to find what may be faint and small features in a complex visual environment, and interpretive skills to rate their (the features') significance [19]. Computing systems are more consistent in their perceiving ability but they cannot match human interpretive skills. Drawing a line so as to limit the system's interpretive function has the virtue of achieving a complementary synthesis of system and radiologists' strengths [20]. However in practice the question of where to draw the line in computer aided detection/diagnostic systems between perception and interpretation is problematic [21].

The HCS process based CAM system developed in this study might be able to address the above problem. Work is in progress to establish whether the HCS based CAM system augments the diagnostic capabilities of the radiologists.

## References

- [1] P. Arbelaez. Boundary Extraction in Natural Images Using Ultrametric Contour Maps. *Proceedings 5th IEEE Workshop on Perceptual Organization in Computer Vision (POCV'06)*. June 2006. New York, USA.
- [2] A. N. Selvan. Highlighting Dissimilarity in Medical Images Using Hierarchical Clustering Based Segmentation (HCS). *M. Phil. dissertation*, Faculty of Arts Computing Engineering and Sciences Sheffield Hallam Univ., Sheffield, UK, 2007.
- [3] R. Ohlander, K. Price, and R. Reddy. Picture segmentation by a recursive region splitting method *Computer Graphics Image Processing*, 8:313-333, 1978.
- [4] M. Nadler, and E. P. Smith. *Pattern Recognition Engineering* John Wiley and Sons inc. 1993.
- [5] P. Schroeter J. Bigün Hierarchical image segmentation by multi dimensional clustering and orientation-adaptive boundary refinement, *Pattern Recognition*, Vol. 28, No. 5, pp. 695-709 1995;
- [6] M. Jeon, M. Alexander, W. Pedrycz and N. Pizzi Unsupervised hierarchical image segmentation with level set and additive operator splitting, *Pattern Recognition Letter* 26 1461-1469 2005.
- [7] H. Zhou, G. Schaefer, A. Sadka and M.E. Celebi Anisotropic mean shift based fuzzy C-means segmentation of dermoscopy images *IEEE Journal of Selected Topics in Signal Processing*, Vol. 3, No. 1, 26-34, 2009.
- [8] H. D. Cheng and Ying Sun, A hierarchical approach to color image segmentation using homogeneity, *IEEE Transactions on Image Processing*, VOL. 9, NO. 12, 2071-2082, 2000.
- [9] C. Thies, A. Malik, D. Keysers, M. Kohnen, B. Fischer and T.M. Lehmann, Content-based retrieval in medical image databases by hierarchical feature clustering, *Procs SPIE 2003*; 5032: 598-608. 2003.
- [10] U. Bhattacharya, B. B. Chaudhuri, S. K. Parui, An MLP-based texture segmentation method without selecting a feature set *Image and Vision Computing* 15 937-948, 1997.
- [11] D. Martin, C. Fowlkes, D. Tal, and J. Malik. A database of human segmented natural images and its application to evaluating segmentation algorithms and measuring ecological statistics *International Conference on Computer Vision*, Vancouver, Canada. 2001.
- [12] Pablo Arbelaez, Charless Fowlkes and David Martin., The Berkeley Segmentation Dataset and Benchmark June, 2007. <http://www.eecs.berkeley.edu/Research/Projects/CS/vision/bsds/>

- [13] Piotr Dollar, Zhuowen Tu, and Serge Belongie, Supervised Learning of Edges and Object Boundaries, *IEEE Computer Vision and Pattern Recognition (CVPR)*, June, 2006.
- [14] Stella X. Yu Segmentation Induced by Scale Invariance *IEEE Conference on Computer Vision and Pattern Recognition*, San Diego, CA, June 20-26, 2005.
- [15] M. Sonka, and J. M. Fitzpatrick. *Handbook of Medical Imaging Volume 2 Medical Image Processing and Analysis*. Published by SPIE-The international society for optical engineering. 2000..
- [16] J. C. Tilton. Hierarchical Image Segmentation *On-line Journal of Space Communication Issue No. 3 Winter 2003 Research and Applications*.
- [17] A. L. Elter M, A. Horsch. CADx of mammographic masses and clustered microcalcifications: a review. *Medical Physics* 2009 Jun;36(6):2052-68. 2009.
- [18] J. Suckling, J. Parker, DR. Dance, S. Astley, I. Hutt, C. Boggis, I. Ricketts, E. Stamatakis, N. Cerneaz, SL. Kok, P. Taylor, D. Betal, and J. Savage. The Mammographic Image Analysis Society Digital Mammogram Database. *Exerpta Medica. International Congress Series* 1069 pp375-378, 1994. <http://peipa.essex.ac.uk/info/mias.html>
- [19] Tabar L. and Dean P;. *Teaching atlas of Mammography* New York: Thieme,1985.
- [20] E. Claridge, Experts' assessment as a "gold standard" for characterization of lesions, *In proceedings of Medical Image Analysis and Understanding Oxford 1997*.
- [21] M. Hartswood, R. Procter, L. Williams, R. Prescott. and P. Dixon, Drawing the line between perception and interpretation in computer-aided mammography *In:Proceedings of the First International Conference on Allocation of Functions: Allocation of Functions*; 01 Oct 1997-03 Oct 1997; Galway. International Ergonomics Association Press; 1997. p. 275-291